

**Electronic supplementary information for**

**Selective hydroconversion of coconut oil-derived lauric acid to alcohol and aliphatic alkanes over MoO<sub>x</sub>-modified Ru catalysts under mild conditions**

**Rodiansono,<sup>a,b\*</sup> Heny Puspita Dewi,<sup>a,b</sup> Kamilia Mustikasari,<sup>a</sup> Maria Dewi Astuti,<sup>a</sup> Sadang Husain,<sup>c</sup> Sutomo<sup>d</sup>**

<sup>a</sup> Department of Chemistry, Faculty of Mathematics and Natural Sciences, Lambung Mangkurat University, Jl. A. Yani Km 36.0 Banjarbaru South Kalimantan, Indonesia.

<sup>b</sup> Catalysis for Sustainable Energy and Environment (CATSuRe), Lambung Mangkurat University.  
e-mail: [rodiansono@ulm.ac.id](mailto:rodiansono@ulm.ac.id) Tel./Fax.: +625114773112

<sup>c</sup> Department of Physics, Faculty of Mathematics and Natural Sciences, Lambung Mangkurat University

<sup>d</sup> Department of Pharmacy, Faculty of Mathematics and Natural Sciences, Lambung Mangkurat University

Contents:

- 1) Physicochemical properties of the synthesised Ru-(y)MoO<sub>x</sub>/TiO<sub>2</sub> catalysts (Tabe 1)
- 2) XRD patterns of Ru-(y)MoO<sub>x</sub>/TiO<sub>2</sub> catalysts before and after reduction with H<sub>2</sub> at 300-600°C for 3 h
- 3) XRD patterns of recovered Ru-(0.026)MoO<sub>x</sub>/TiO<sub>2</sub> catalyst
- 4) TEM images of Ru-(0.026)MoO<sub>x</sub>/TiO<sub>2</sub> catalyst before reaction and recovered
- 5) Typical GC chart of reaction results of hydroconversion of lauric acid to lauryl alcohol and alkane using Ru–MoO<sub>x</sub>/TiO<sub>2</sub> catalysts

The physico-chemical properties such as specific surface area BET ( $S_{\text{BET}}$ ), average Ru particle sizes, total acidity, and  $\text{H}_2$  uptake of Ru-MoO<sub>x</sub>/TiO<sub>2</sub> are summarized in **Table S1**.

**Table S1** Physico-chemical properties of Ru-MoO<sub>x</sub>/TiO<sub>2</sub> catalyst

Entry	Catalyst	Mo loading amount (mmol g <sup>-1</sup> )	$S_{\text{BET}}^a$ (m <sup>2</sup> /g)	$V_{\text{pore}}^a$ (cm <sup>3</sup> /g)	$D^b$ (nm)	Total Acid <sup>c</sup> (μmol NH <sub>3</sub> /g)
1	Ru-(0.011)MoO <sub>x</sub> /TiO <sub>2</sub>	0.011	23.7	0.035	nd	223
2 <sup>d</sup>	Ru-(0.026)MoO <sub>x</sub> /TiO <sub>2</sub>	0.026	20.8	0.029	3.48	199
3	Ru-(0.049)MoO <sub>x</sub> /TiO <sub>2</sub>	0.049	21.3	0.033	nd	201
4	Ru-MoO <sub>x</sub> /TiO <sub>2</sub>	0.026	19.8	0.031	3.48	298
5	Ru-MoO <sub>x</sub> /TiO <sub>2</sub> [recovered]	0.026	20.4	0.034	n.a.	n.a.

<sup>a</sup> $S_{\text{BET}}$  is specific surface areas, determined by N<sub>2</sub> physisorption at 77 K using BET method. <sup>b</sup>Average particle sizes of Ru derived from TEM images. <sup>c</sup>Acidity was derived from NH<sub>3</sub>-TPD spectra. <sup>d</sup>Recovered catalyst after the second reaction of lauric acid hydroconversion.

The XRD analysis of H<sub>2</sub>-activated Ru-(0.026)MoO<sub>x</sub>/TiO<sub>2</sub> at 400°C and 500°C (Fig. S1) unable to detect the formations of metallic Ru or bimetallic Ru-MoO<sub>x</sub> phase due to its extremely very small the Ru particle sizes.

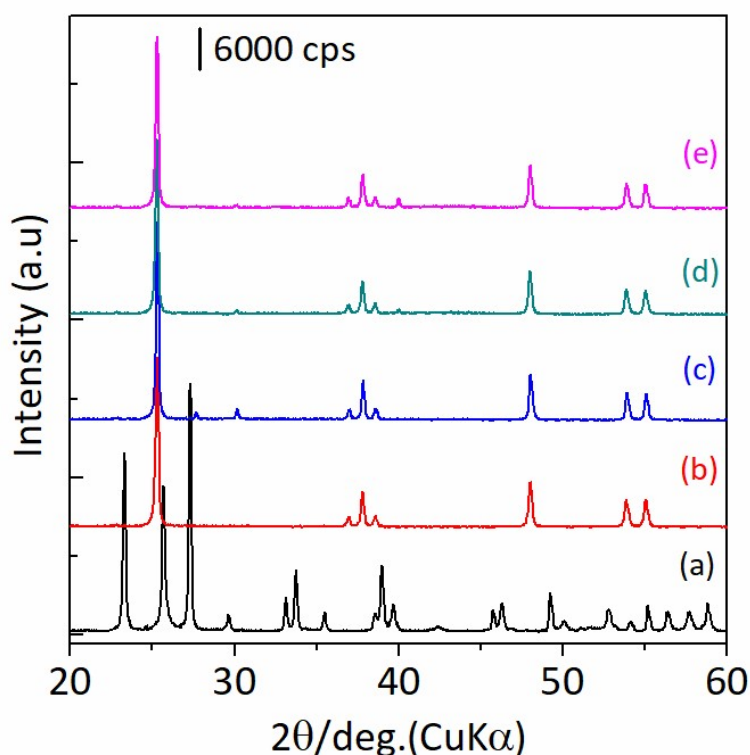


**Fig. S1** XRD patterns of (a) 5wt%Ru@MoO<sub>3</sub>, (b) 5wt%Ru/TiO<sub>2</sub>, and Ru-(y)MoO<sub>x</sub>/TiO<sub>2</sub> with different Mo loading amount of (c) 0.011 mmol g<sup>-1</sup>, (d) 0.026 mmol g<sup>-1</sup>, and (e) 0.049 mmol g<sup>-1</sup> after reduction with H<sub>2</sub> at 400°C for 3 h.

A typical TEM images of H<sub>2</sub>-reduced Ru-(0.026)MoO<sub>x</sub>/TiO<sub>2</sub> at 400°C for 1.5 h showed the dispersed both Ru and Mo species on surface of TiO<sub>2</sub> and the estimated particle sizes of metallic Ru were around 3.48 nm as indicated in Fig. S2.

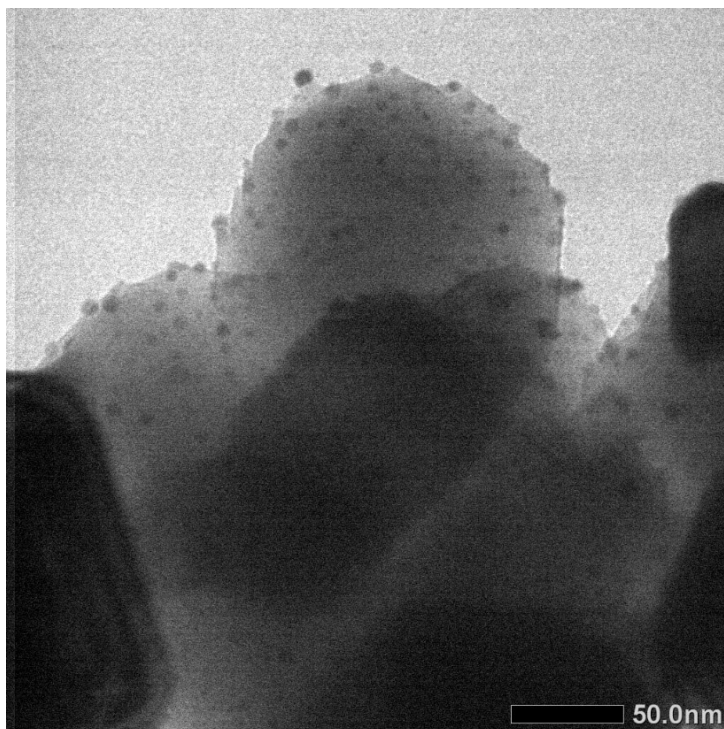


**Fig. S2** Typical TEM images of Ru-(0.026)MoO<sub>x</sub>/TiO<sub>2</sub> catalyst after reduction with H<sub>2</sub> at 400°C for 3 h.

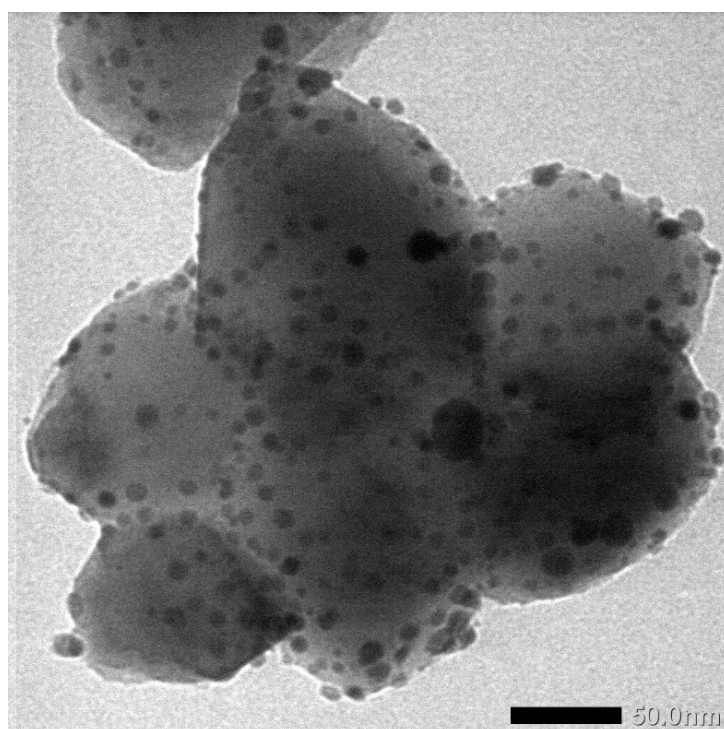


**Fig. S3** Typical TEM images of Ru-(0.049)MoO<sub>x</sub>/TiO<sub>2</sub> catalyst after reduction with H<sub>2</sub> at 400°C for 3 h.

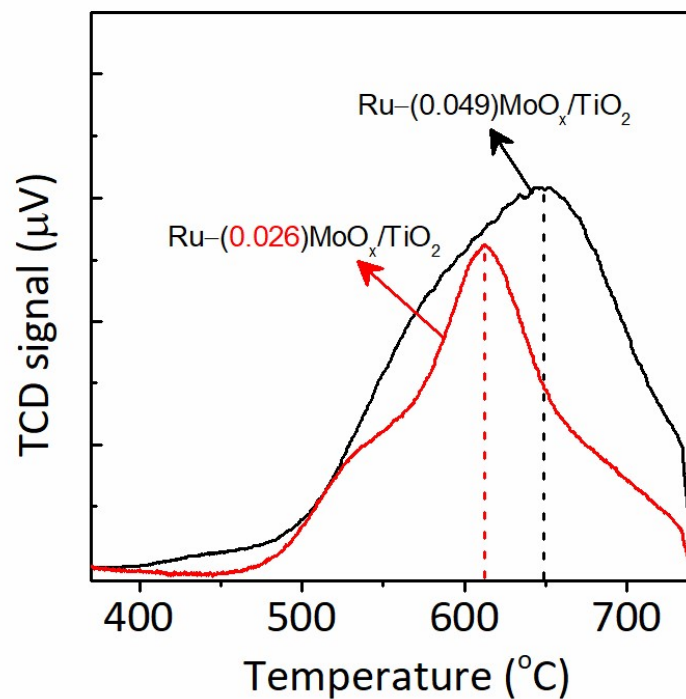


**Fig. S4** NH<sub>3</sub>-TPD profiles of Ru-MoO<sub>x</sub>/TiO<sub>2</sub> with different Mo loading amount of 0.026 mmol g<sup>-1</sup> and 0.049 mmol g<sup>-1</sup> catalysts after reduction with H<sub>2</sub> at 400°C for 3 h.

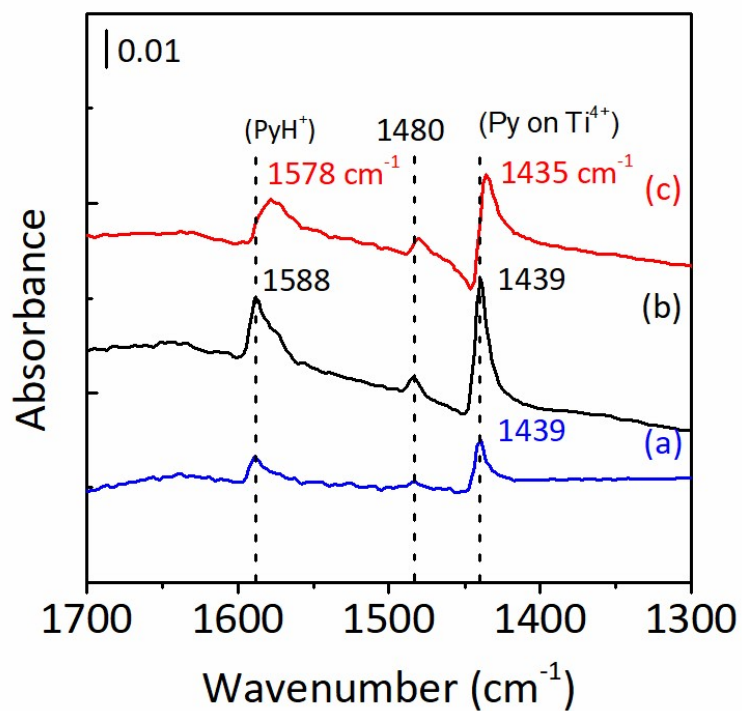


**Fig. S5** Pyridine adsorption profiles of (a) 5wt%Ru/TiO<sub>2</sub>, (b) Ru-(0.026)MoO<sub>x</sub>/TiO<sub>2</sub>, (c) Ru-(0.049)MoO<sub>x</sub>/TiO<sub>2</sub> catalysts after reduction with H<sub>2</sub> at 400°C for 3 h.

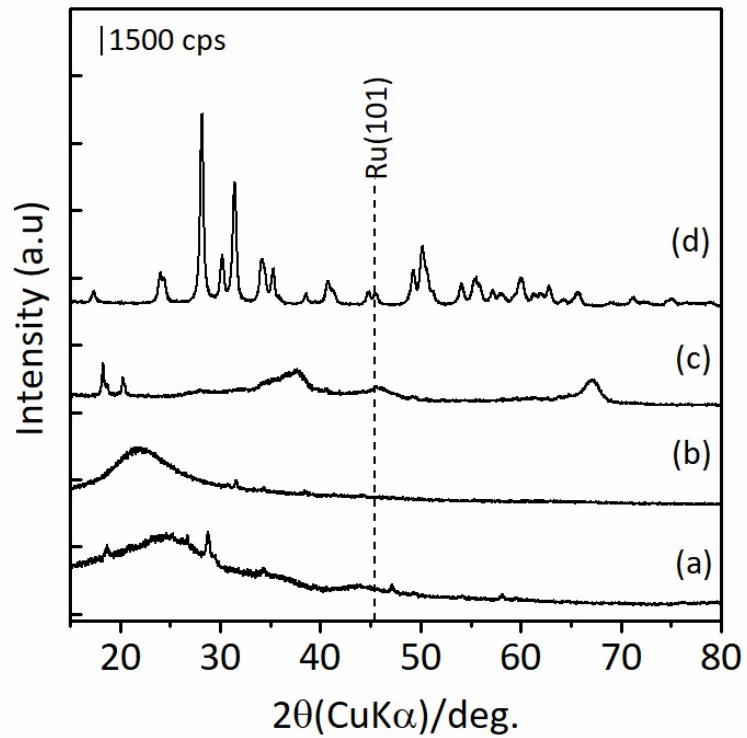


**Fig. S6** XRD patterns of Ru–MoO<sub>x</sub> supported on (a) SiO<sub>2</sub>, (b) charcoal (active carbon), (c) γ–Al<sub>2</sub>O<sub>3</sub>, and (d) ZrO<sub>2</sub> catalysts after reduction with H<sub>2</sub> at 400°C for 3 h.

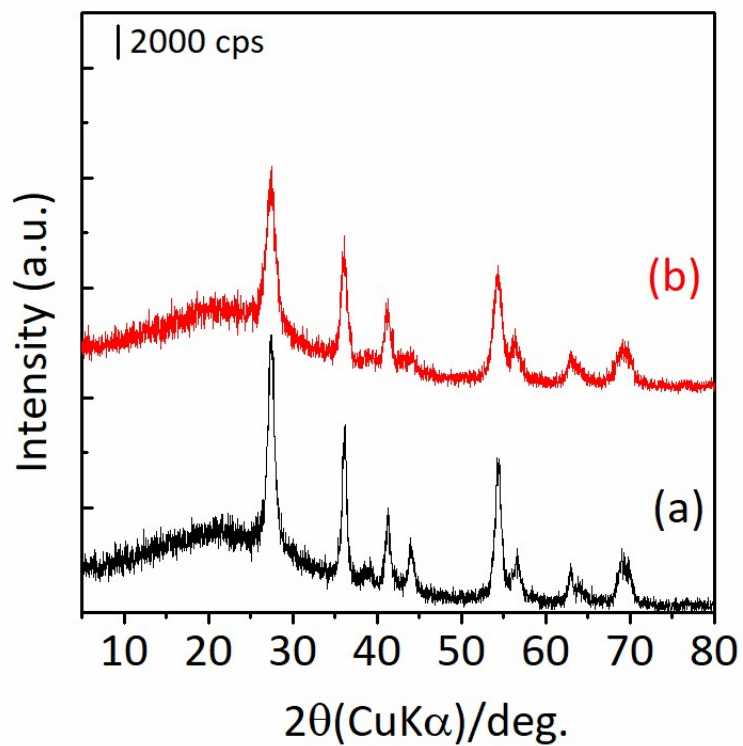


**Fig. S7** XRD patterns of Ru–MoO<sub>x</sub>/C–TiO<sub>2</sub> (a) as-prepared and (b) after reduction with H<sub>2</sub> at 400°C for 3 h.

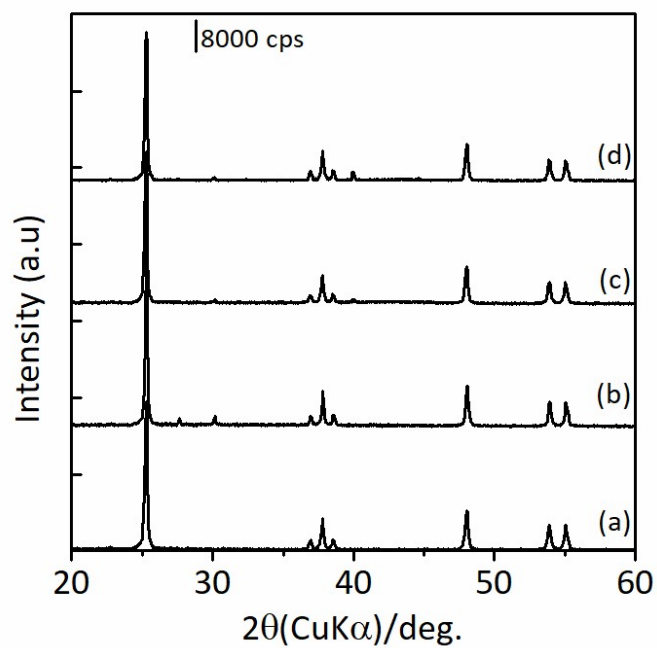


**Fig. S8** XRD patterns of (a) Ru(5wt%)/TiO<sub>2</sub> anatase and Ru-(0.026)MoO<sub>x</sub>/TiO<sub>2</sub> after reduction with H<sub>2</sub> at different temperature of (b) 400°C, (c) 500°C and (d) 600°C for 3 h.

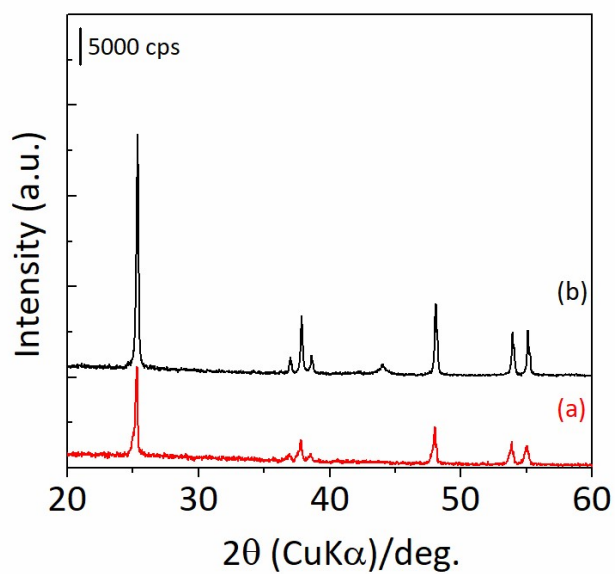


**Fig. S9** XRD patterns of recovered Ru-(0.026)MoO<sub>x</sub>/TiO<sub>2</sub> (500°C/H<sub>2</sub>) catalyst after the 2<sup>nd</sup> recycled reaction run.

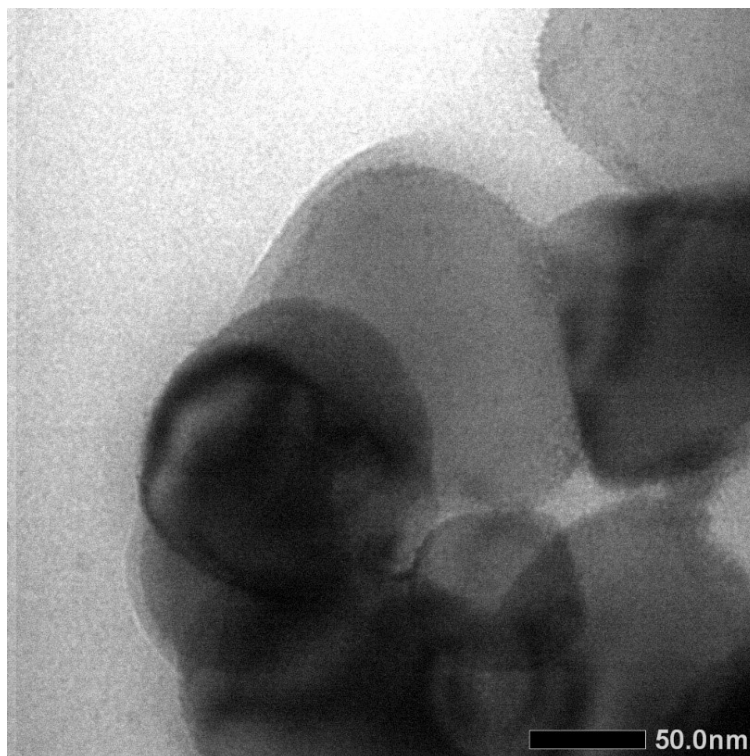


**Fig. S10** Typical TEM images of recovered Ru-(0.026)MoO<sub>x</sub>/TiO<sub>2</sub> (500°C/H<sub>2</sub>) catalyst after the 2<sup>nd</sup> recycled reaction run.

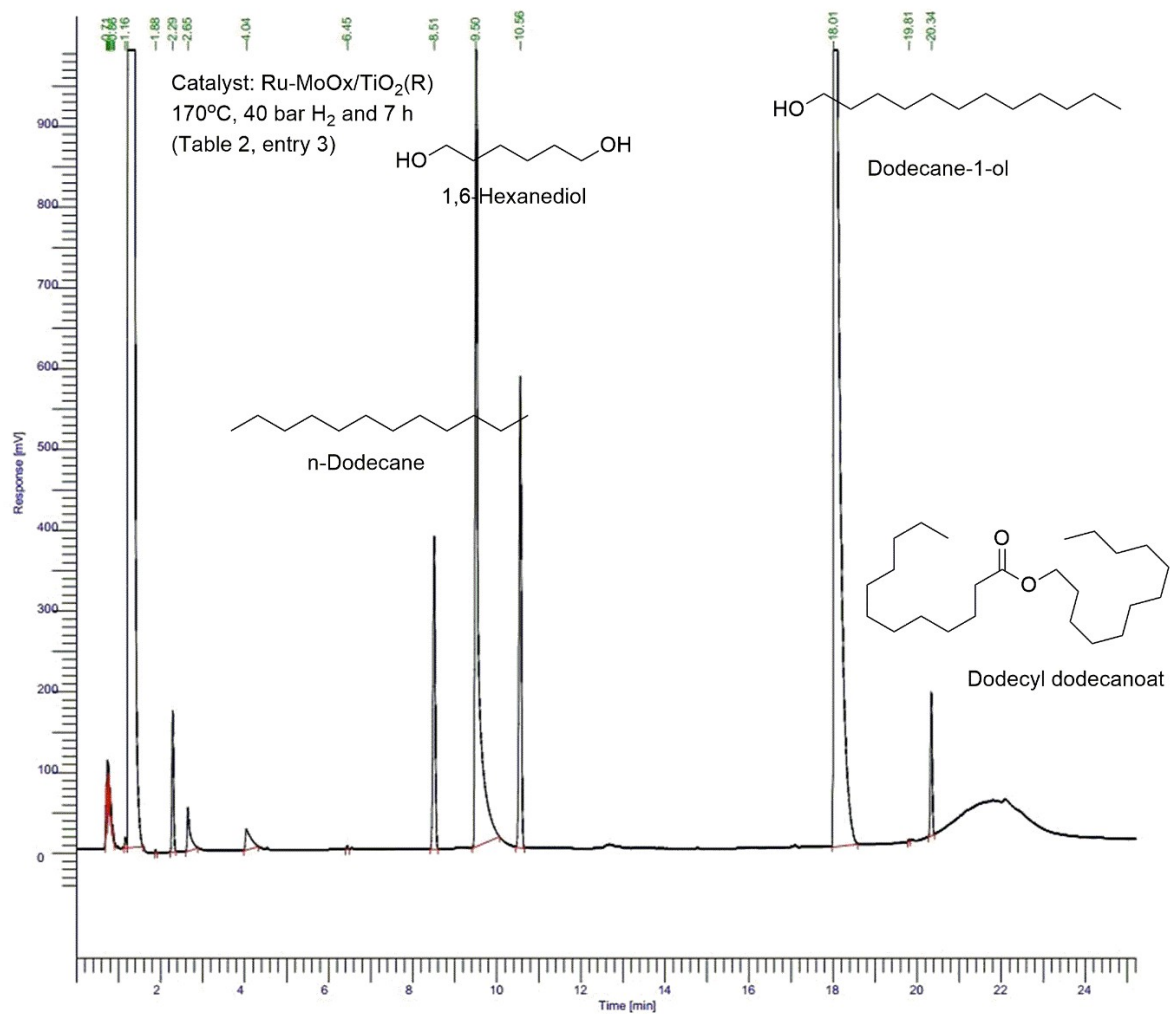


Fig. S11 Typical GC chart of reaction results of hydroconversion of lauric acid to lauryl alcohol and alkane using Ru-MoO<sub>x</sub>/TiO<sub>2</sub> (R) catalyst (Table 2. Entry 3).



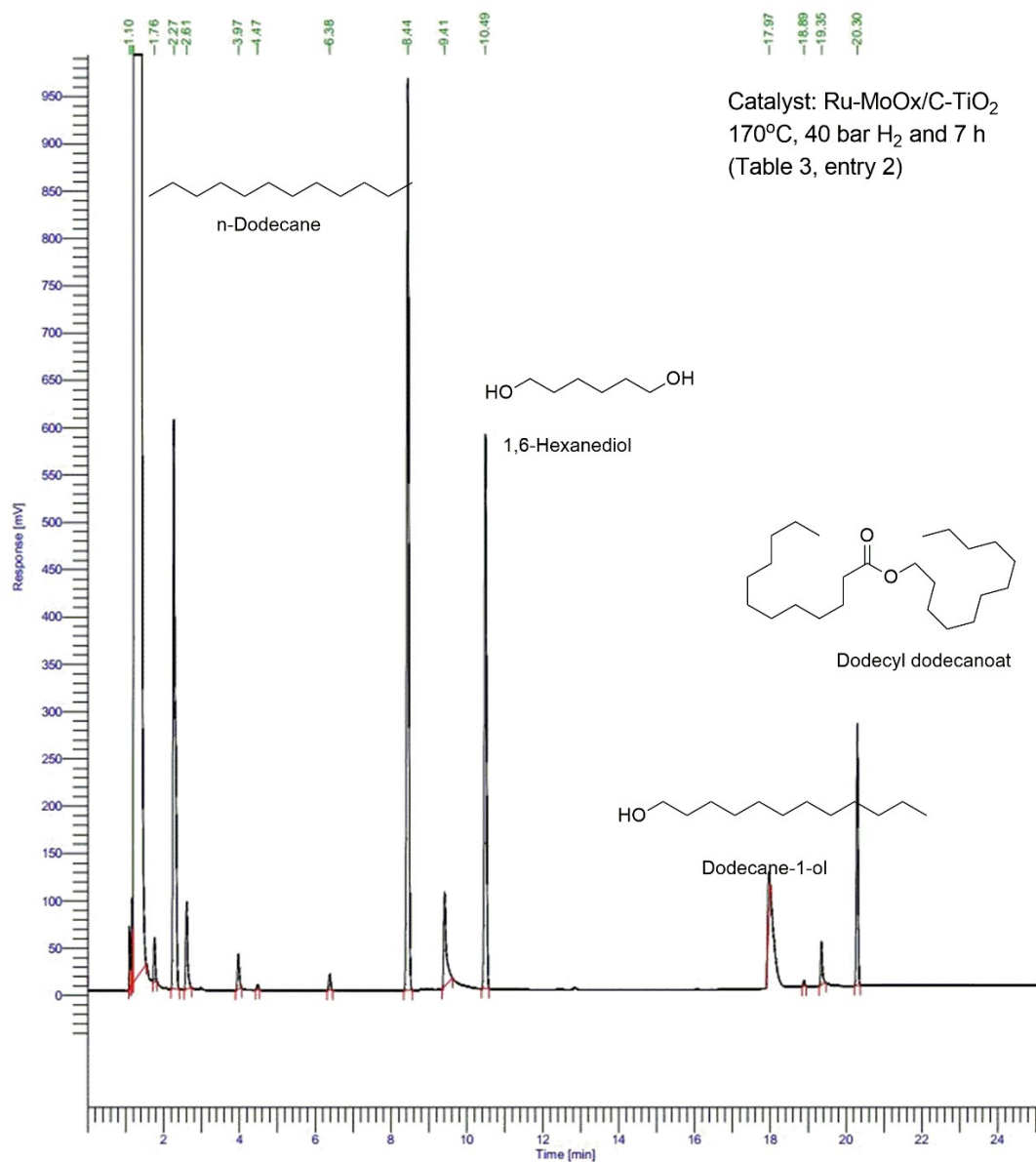


Fig. S12 Typical GC chart of reaction results of hydroconversion of lauric acid to lauryl alcohol and alkane using Ru-MoO<sub>x</sub>/C-TiO<sub>2</sub> catalyst (Table 3, entry 2).

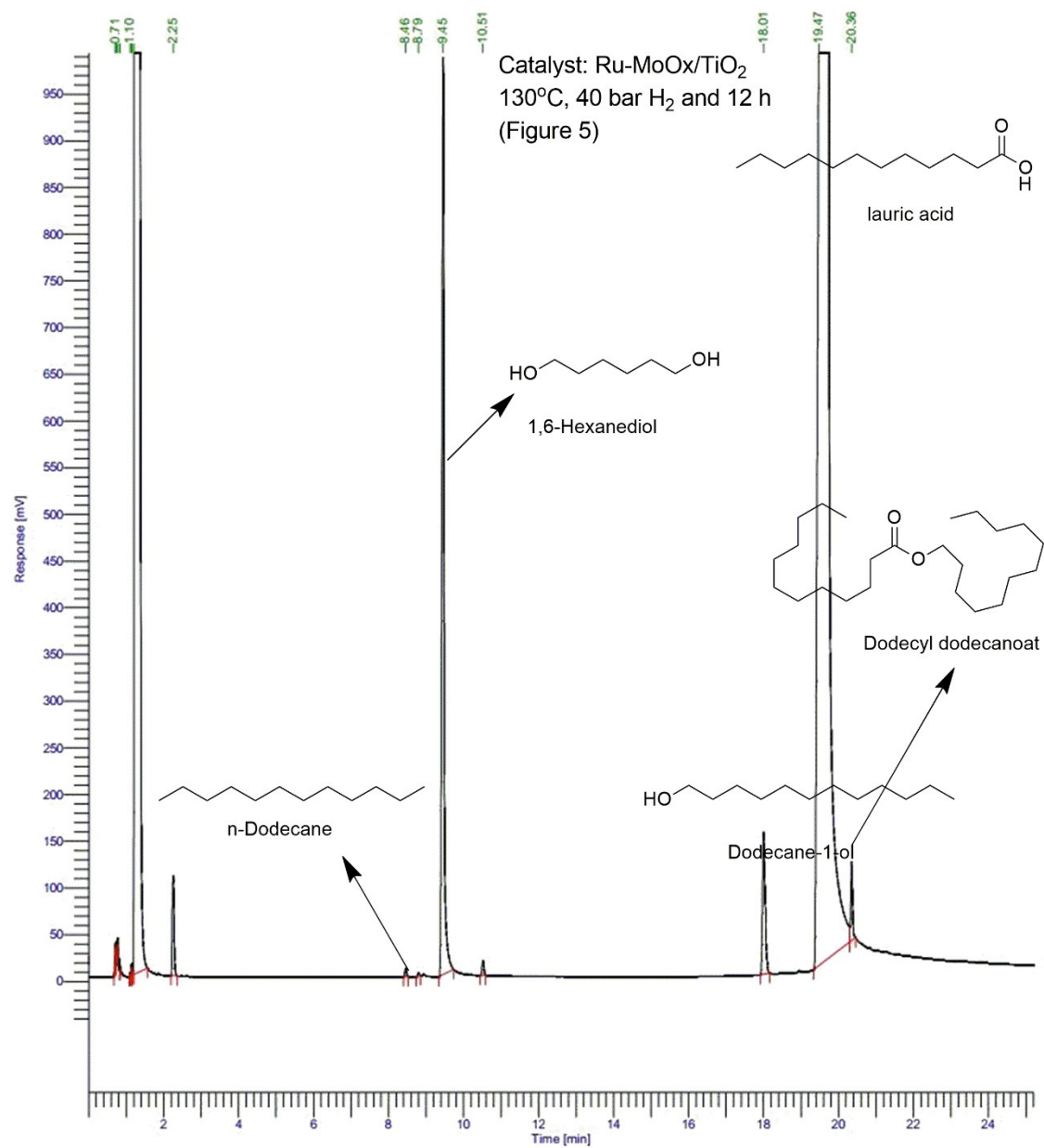


Fig. S13 Typical GC chart of reaction results of hydroconversion of lauric acid to lauryl alcohol and alkane using Ru-MoO<sub>x</sub>/TiO<sub>2</sub> catalyst (Figure 5, 130°C, 40 bar, 12 h). Conversion (58%), Yield of dodecane-1-ol (20.2%), yield of n-dodecane (2%), and yield of dodecyl dodecanoate (35.7%).